LETTER Communicated by Mike Arnold

Recurrent Cerebellar Loops Simplify Adaptive Control of Redundant and Nonlinear Motor Systems

John Porrill
j.porrill@sheffield.ac.uk
Paul Dean
P.Dean@sheffield.ac.uk
Centre for Signal Processing in Neuroimaging and Systems Neuroscience, Department of Psychology, University of Sheffield, Sheffield S10 2TP, U.K.

We have described elsewhere an adaptive filter model of cerebellar learning in which the cerebellar microcircuit acts to decorrelate motor commands from their sensory consequences (Dean, Porrill, & Stone, 2002). Learning stability required the cerebellar microcircuit to be embedded in a recurrent loop, and this has been shown to lead to a simple and modular adaptive control architecture when applied to the linearized 3D vestibular ocular reflex (Porrill, Dean, & Stone, 2004). Here we investigate the properties of recurrent loop connectivity in the case of redundant and nonlinear motor systems and illustrate them using the example of kinematic control of a simulated two-joint robot arm. We demonstrate that (1) the learning rule does not require unavailable motor error signals or complex neural reference structures to estimate such signals (i.e., it solves the motor error problem) and (2) control of redundant systems is not subject to the nonconvexity problem in which incorrect average motor commands are learned for end-effector positions that can be accessed in more than one arm configuration. These properties suggest a central functional role for the closed cerebellar loops, which have been shown to be ubiquitous in motor systems (e.g., Kelly & Strick, 2003).

1 Introduction

The grace and economy of animal movement suggest that neural control methods are likely to be of interest to robotics. The neural structure particularly associated with coordinated movement is the cerebellum, whose function seems to be the fine-tuning of motor skills by elaborating incomplete or approximate commands issued by higher levels of the motor system (Brindley, 1964). But although the microcircuitry of cerebellar cortex has inspired models for over 30 years (Albus, 1971; Eccles, Ito, & Szentágothai, 1967; Marr, 1969), the results appear to have produced relatively meager benefits for robotics. As Marr himself commented, "In my own case, the cerebellar study ... disappointed me, because even if the theory was

correct, it did not enlighten one about the motor system—it did not, for example, tell one how to go about programming a mechanical arm" (Marr, 1982, p. 15).

Part of the problem is that the control function of any individual region of the cerebellum depends not only on its internal microcircuitry but also on the way it is connected with other parts of the motor system (Lisberger, 1998), and in many cases the details of this connectivity are still not well understood. However, recent anatomical investigations have suggested that there may be a common feature of cerebellar connectivity: a recurrent architecture. It appears as if individual regions of the cerebellum (1) receive a copy of the low-level motor commands that constitute system output and (2) apply their corrections to the high-level command. These "multiple closed-loop circuits represent a fundamental architectural feature of cerebro-cerebellar interactions," and it is a challenge to future studies to "determine the computations that are supported by this architecture" (Kelly & Strick, 2003). Determining these computations might also throw light on how biological control methods using the cerebellum might be of use to robotics.

Our initial attempts to address this issue considered adaptation of the angular vestibular-ocular reflex (aVOR), a classic preparation for studying basic cerebellar function (Boyden, Katoh, & Raymond, 2004; Carpenter, 1988; Ito, 1970). In this reflex, a head-rotation signal from vestibular sensors is used to counter-rotate the eye to maintain stability of the retinal image. Visual processing delays of ~100 ms mean that movement of the retinal image (a retinal slip) is used as an error signal for calibration of the aVOR rather than for online control, and this calibration requires the floccular region of the cerebellum. In our simulations of the aVOR, the characteristics of the oculomotor plant (eye muscles plus orbital tissue) were altered, and the flocculus (modeled as an adaptive filter; see section 2) was required to learn the appropriate plant compensation. Stable and robust learning was achieved by connecting the filter so that it decorrelated the retinal slip signal from a copy of the motor command sent to the eye muscles (Dean, Porrill, & Stone, 2002; Porrill, Dean, & Stone, 2004) and sent its output to join the vestibular input. This arrangement constitutes an example of the recurrent architecture described above, and ensuring the stability of the decorrelation control algorithm is therefore a candidate for its computational role.

Here we extend these findings to derive some theoretical properties of the recurrent cerebellar architecture, which indicate that it may play a central role in simplifying the adaptive control of nonlinear and redundant biological motor systems. These properties will be illustrated by comparison of forward and recurrent architectures in simulated calibration of the inverse kinematic control of a two-degree-of-freedom (2dof) robot arm.

Part of this work has been reported in abstract form (Porrill & Dean, 2004).

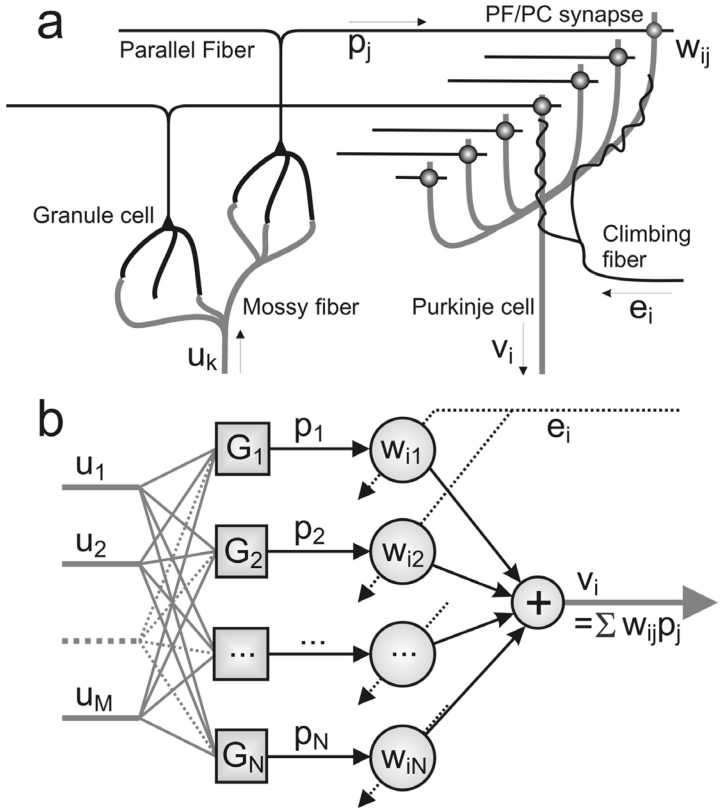

Figure 1: (a) Schematic representation of the cerebellar microcircuit. MF inputs u_k are analyzed in the granule cell layer (only one MF input is shown; in reality, GCs receive direct input from multiple MFs and indirect input from many more via recurrent connections, not shown here, to PFs), and the GC output signals p_j are distributed along the PFs. The ith PC makes contact with many PFs that drive its simple spike output v_i. The cell also has a CF input e_i, which is assumed in Marr-Albus models to act as a teaching signal for the synaptic weights w_{ij}. (b) Interpretation of the cerebellar microcircuit as an adaptive filter. Granule cells processing is modeled as a filter $p_i = G_i(u_1, u_2, \ldots)$, and each PC outputs a weighted sum of its PF inputs. (Figure modified from Dean, Porrill, & Stone, 2004.)

2 The Adaptive Filter Model

We will use what is perhaps the simplest implementation of the Marr-Albus architecture: the adaptive filter (Fujita, 1982). The microcircuit based around a Purkinje cell (PC) and its computational interpretation as an adaptive filter model are shown schematically in Figure 1.

The mossy fibers (MFs) carry input signals ($u_1, u_2, \ldots$) that are processed in the granule cell layer to produce the signals ($p_1, p_2, \ldots$) carried on the parallel fibers (PFs). This process is interpreted as a massive expansion-recoding of the mossy fiber inputs of the form

$$p_j = G_j(u_1, u_2, \ldots). \tag{2.1}$$

In the nondynamic problems to be considered here, the G_j are functions of the current values of ($u_1, u_2, \ldots$). Dynamic problems can be tackled by allowing the p_j to encode aspects of the past history of the u_i; in that case, the G_j are required to be more general causal functionals such as tapped delay lines.

We are interested in the output of a subset of Purkinje cells that take their inputs from common parallel fibers. The output v_i of the ith such PC is modeled as a weighted linear combination of its PF inputs,

$$v_i = \sum w_{ij} p_j, \tag{2.2}$$

where the coefficient w_{ij} is the synaptic weight of the jth PF on the ith PC.

The combined transformation from the vector of inputs $\mathbf{u} = (u_1, u_2, \ldots)$ to the vector of outputs $\mathbf{v} = (v_1, v_2, \ldots)$ can then be written conveniently as a vector equation,

$$\mathbf{v} = \mathbf{C}(\mathbf{u}) = \sum w_{ij} \mathbf{G}_{ij}(\mathbf{u}), \tag{2.3}$$

where $\mathbf{G}_{ij}(\mathbf{u}) = (0, \ldots, G_j(\mathbf{u}), \ldots, 0)$ is the vector with the jth parallel fiber signal as its ith entry and zeros elsewhere.

In Marr-Albus models, the climbing fiber input e_i to the Purkinje cell is assumed to act as a teaching signal. The qualitative properties of long-term depression (LTD) and long-term potentiation (LTP) at PF/PC synapses are consistent with the anti-Hebbian heterosynaptic covariance learning rule (Sejnowski, 1977),

$$\delta w_{ij} = -\beta \langle e_i \; p_j \rangle, \tag{2.4}$$

which is identical in form to the least mean square (LMS) learning rule of adaptive control theory (Widrow & Stearns, 1985). Note that in all the above formulas, neural signals are assumed to be coded as firing rates relative to a tonic firing rate, and hence can take both positive and negative values.

3 Example Problem: Learning Inverse Kinematics

We will show that recurrent loops can simplify the adaptive control of nonlinear and redundant motor systems. We derive the results for a problem

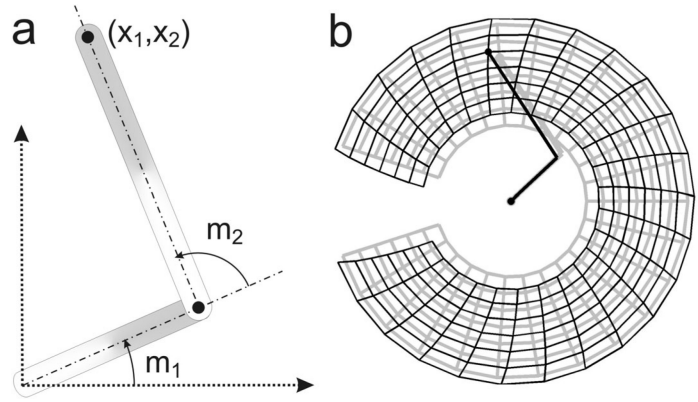

Figure 2: (a) Geometry of the planar, two-degree-of-freedom robot arm. Motor commands (m_1, m_2) specify joint angles as shown. The position (x_1, x_2) of the end effector is specified in Cartesian coordinates in arbitrary units. (b) Example plant compensation problem. The arm controller is initially calibrated for the arm lengths $l_1 = 1.1, l_2 = 1.8$ of the gray arm. This arm is shown reaching accurately to a point on the gray polar grid covering the work space. When used with the black arm (lengths $l_1 = 1, l_2 = 2$), this approximate controller reaches to points on the distorted (black) grid. The task of the cerebellum is to compensate for this miscalibration; reaching errors $(\delta x_1, \delta x_2)$ are provided in Cartesian coordinates.

presenting both of these difficulties: learning robot inverse kinematics. This problem is of general interest, since it is an equivalent to the generic problem of learning right inverse mappings. The theoretical results obtained in the general case will be illustrated throughout by application to the inverse kinematic problem for the 2dof robot arm shown in Figure 2, where the geometry is particularly easy to intuit. Although this is a very simple system, it exhibits strong nonlinearity and a discrete redundancy. We begin by recalling some terminology.

The forward kinematics or plant model of a robot arm is the mapping $\mathbf{x} = \mathbf{P}(\mathbf{m})$ from motor commands $\mathbf{m} = (m_1, \ldots, m_M)$ to the end-effector positions $\mathbf{x} = (x_1, \ldots, x_S)$. An inverse kinematics is a mapping $\mathbf{m} = \mathbf{Q}(\mathbf{x})$ that calculates the motor commands corresponding to a given end-effector position. Since this implies that $\mathbf{x} = \mathbf{P}(\mathbf{Q}(\mathbf{x}))$, an inverse kinematics is a right-inverse $\mathbf{P}^{-1}$ for $\mathbf{P}$. For redundant systems, a given position can be reached using more than one choice of motor command; in this case, we will use the notation $\mathbf{Q} = \mathbf{P}^{-1}$ to denote a particular choice of inverse kinematics. For the 2dof arm, there are only two choices of motor command for a given end-effector position. This is an example of a discrete redundancy. More complex systems can have continuous redundancies in which there is a

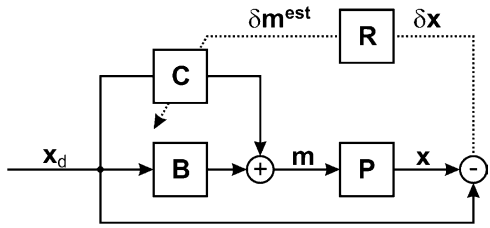

Figure 3: Forward architecture. The desired position input $\mathbf{x}_d$ produces a motor command $\mathbf{m} = \mathbf{B}(\mathbf{x}_d) + \mathbf{C}(\mathbf{x}_d)$, which is the sum of contributions from a fixed element **B** and an adaptive cerebellar element **C**. This input to the plant **P** produces the output position **x**. Training the weights of **C** requires proximal or motor error $\delta\mathbf{m}$ rather than distal or sensory error $\delta\mathbf{x} = \mathbf{x} - \mathbf{x}_d$. Hence, in this forward architecture, motor error must be estimated by backpropagation via a reference matrix $\mathbf{R} \approx \partial\mathbf{P}^{-1}/\partial\mathbf{x}$. This requires detailed prior knowledge of the motor plant.

continuum of motor commands available for each end-effector position. These are sometimes called redundant degrees of freedom.

The cerebellum has been described as a "repair shop," compensating for miscalibration (due to damage, fatigue, or development, for example) of the motor plant (Robinson, 1974). It is this adaptive plant compensation problem that we will model here; that is, we assume that an approximate inverse kinematics controller $\mathbf{B} \approx \mathbf{P}^{-1}$ is available to the system and that the function of the cerebellum is to supplement this controller to produce more accurate movements. Learning is supervised by making the reaching error,

$$\delta\mathbf{x} = \mathbf{x} - \mathbf{x}_d = \mathbf{P}(\mathbf{B}(\mathbf{x}_d)) - \mathbf{x}_d, \tag{3.1}$$

available to the learning system, where $\mathbf{x}_d$ is the target (desired) position. We call this quantity *sensory error* since it can be measured by an appropriate sensor and to distinguish it from motor error, which will be defined later.

In the 2dof robot arm example shown in Figure 2b, the approximate controller **B** is the inverse kinematics for a robot with arm lengths that are $\pm 10\%$ in error. Thus, when required to reach to positions on the polar grid shown in Figure 2, the arm actually moves to positions on the overlaid distorted grid.

4 The Forward Learning Architecture

To highlight the properties of recurrent connectivity, we begin by considering the problems encountered in implementing a learning rule for the alternative forward connectivity shown schematically in Figure 3. The motor command to the plant is produced by an open-loop filter that is the sum

$\mathbf{B} + \mathbf{C}$ of the fixed element $\mathbf{B}$ and the adaptive cerebellar component $\mathbf{C}$; this combination will be an inverse kinematics $\mathbf{B} + \mathbf{C} = \mathbf{P}^{-1}$ if $\mathbf{C}$ takes the value

$$\mathbf{C}^* = \sum w_{ij}^* G_{ij} = \mathbf{P}^{-1} - \mathbf{B}. \tag{4.1}$$

We assume that the granule cell basis functions $\mathbf{G}_{ij}$ satisfy the matching condition, that is, that synaptic weights w_{ij}^* can be found such that the above equation holds for the range of $\mathbf{P}^{-1}$ and $\mathbf{B}$ under consideration.

To obtain a learning rule similar to the covariance rule (see equation 2.3), we introduce the concept of motor error (Gomi & Kawato, 1992). Motor error $\delta\mathbf{m}$ is the error in motor command responsible for the sensory error $\delta\mathbf{x}$. Minimizing expected square motor error,

$$E_m = \frac{1}{2}\left\langle \delta m^2 \right\rangle = \frac{1}{2}\left\langle \delta\mathbf{m}^t \delta\mathbf{m} \right\rangle, \tag{4.2}$$

(where a superscript t denotes the matrix transpose), leads to a simple learning rule because motor error is linearly related to synaptic weight error,

$$\delta\mathbf{m} = \mathbf{C}(\mathbf{x}_d) - \mathbf{C}^*(\mathbf{x}_d) = \sum (w_{ij} - w_{ij}^*)\mathbf{G}_{ij}(\mathbf{x}_d). \tag{4.3}$$

Using this expression, the gradient of expected square motor error is

$$\frac{\partial E}{\partial w_{ij}} = \left\langle \delta\mathbf{m}^t \frac{\partial \delta\mathbf{m}}{\partial w_{ij}} \right\rangle = \left\langle \delta\mathbf{m}^t \mathbf{G}_{ij}(\mathbf{x}_d) \right\rangle = \left\langle \delta m_i \, p_j \right\rangle, \tag{4.4}$$

giving the gradient descent learning rule,

$$\delta w_{ij} = -\beta \left\langle \delta m_i \, p_j \right\rangle, \tag{4.5}$$

where β is a small, positive constant. If we label Purkinje cells such that the ith PC output contributes to the ith component of motor error, then comparison with the covariance learning rule (see equation 2.4) shows that the teaching signal e_i provided on the climbing fiber input to the ith Purkinje cell must be the ith component of motor error,

$$e_i = \delta m_i. \tag{4.6}$$

This apparently simple prescription is complicated by the fact that motor error is not in itself an observable quantity. It is a derived quantity given by the equation

$$\delta\mathbf{m} = \mathbf{P}^{-1}(\mathbf{x}) - \mathbf{P}^{-1}(\mathbf{x}_d). \tag{4.7}$$

This leads to an obvious circularity in that the rule for learning inverse kinematics requires prior knowledge of that same inverse kinematics. This circularity can be circumvented to some extent by supposing that all errors are small so that

$$\delta \mathbf{m} \approx \frac{\partial \mathbf{P^{-1}}}{\partial \mathbf{x}} \delta \mathbf{x}, \tag{4.8}$$

and then replacing the unknown Jacobian $\partial \mathbf{P}^{-1}/\partial \mathbf{x}$ in this error backpropagation rule by a fixed approximation,

$$R \approx \frac{\partial \mathbf{P^{-1}}}{\partial \mathbf{x}}. \tag{4.9}$$

If R were exact, then, if J is the forward Jacobian $J = \partial \mathbf{P}/\partial \mathbf{m}$, the product JR would be the identity matrix. To ensure stable learning, the approximate R must estimate motor error correctly up to a strict positive realness (SPR) condition, which in this static case requires that the symmetric part of the matrix JR be positive definite. The hypothetical neural structures required to implement this transformation R and recover motor error from observable sensory error,

$$\delta \mathbf{m} \approx R \delta \mathbf{x} \quad \text{or} \quad \delta m_i \approx \sum R_{ik} \delta x_k, \tag{4.10}$$

have been called reference structures (Gomi & Kawato, 1992), so we will call R the reference matrix.

5 The Motor Error Problem

We refer to the requirement that the climbing fibers carry the unobservable motor error signal rather than the observed sensory error signal as the motor error problem. Although the forward architecture has been applied successfully to a number of real and simulated control tasks (notably in the form of the feedback error learning architecture; Gomi & Kawato, 1992, 1993), we will argue here that for generic biological control systems, the complexity of the neural reference structures it requires makes forward architecture implausible.

It is clear that the complexity of the reference structure is multiplicative in the dimension of the control and sensor space. For a task in which M muscles control the output of N sensors, there are MN entries in the reference matrix R. For example, in our 2dof robot arm problem, four real numbers must be hard-wired to guarantee learning. For more realistic motor tasks in biological systems (such as reaching while preserving balance), values of 100 or more for MN would not be unreasonable.

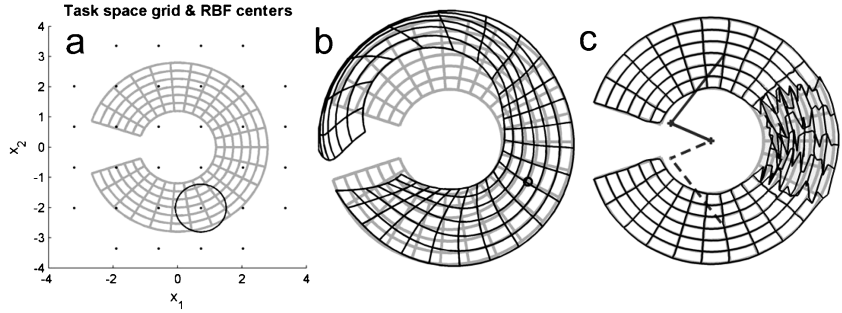

Figure 4: (a) The dots show the arrangement of RBF centers, and the circle shows the receptive field radius for the forward architecture. This configuration leads to an accurate fit if exact motor error is provided to the learning algorithm (not shown). (b) A snapshot of performance during learning that illustrates the need for multiple reference structures in nonlinear problems. The reference structure R is chosen as the exact Jacobian at the grid point marked with a small circle. Although the learned (black) grid overlays the exact (gray) grid more accurately in the neighborhood of O (compare with Figure 3 bottom), performance has clearly deteriorated over the remainder of the work space. Learning rate beta $= 0.0005$. The effect of reducing the learning rate is to delay but not abolish the divergence. (c) An illustration of the redundancy or nonconvexity problem. The arm controller is set up to consistently choose the configurations shown by the solid and dotted arms when reaching into the top or bottom half of the work space. However, when reaching to points in the shaded horizontal sector, the arm retains the configuration used for the previous target. Hence, arm configuration is chosen effectively randomly in this sector, and the system fails to learn. Learning rate is as above. (Exact motor errors were used in this part of the simulation).

In fact, this analysis understates the problem since biological motor systems are often nonlinear, and hence the reference structures are valid only locally. This behavior will be illustrated for the 2dof robot arm calibration problem described above (see Figure 2). Details of the radial basis function (RBF) implementation are given in the appendix. Figure 4a shows a snapshot of performance during learning. In this example, the reference matrix R was chosen to be the exact inverse Jacobian at the point O. Clearly this choice satisfies the SPR condition in a neighborhood of O, and hence in this region where R provides good estimates of motor error, reaching accuracy initially improves. However, outside this region, the sign of a component of motor error is wrongly estimated, and errors in this component diverge catastrophically. This instability will eventually spread to the point O itself because of overlap between adjacent RBFs.

To ensure stable learning in this example would require at least three reference structures valid on three different sectors of the work space.

This requires $3 \times 4 = 12$ prespecified parameters (not including the extra parameters needed to specify the region of validity of each reference structure). For a general inverse kinematics problem, we must specify MNK parameters, where K is the number of regions required to guarantee that positive definiteness of JR in each region.

Finally, we note that in the dynamic case, learning must be dynamically stable. For example, in the linear case, the required reference structure is a matrix of transfer functions $R(i\omega)$, and an SPR condition must be satisfied by the matrix transfer function $J(i\omega)R(i\omega)$ at each frequency, further increasing the complexity of the motor error problem.

6 The Redundancy Problem

Most artificial and biological motor systems are redundant, that is, different motor commands can produce the same output. Such redundancy leads to a classic supervised learning problem called the nonconvexity problem: if the training data for the learning system associate multiple motor commands with a given position, and if this set of motor commands is nonconvex, then the system will learn an inappropriate weighted average motor command at that position.

The forward architecture shown in Figure 3 is subject to the redundancy problem whenever the controller **B** is allowed to produce different output commands for the same input. This type of behavior is common in motor tasks; for example, a robot arm configuration might be determined by a combination of convenience and movement history.

This type of behavior is illustrated for the 2dof arm in Figure 4b. In this experiment, one arm configuration is used in the top half of the work space and the opposite configuration in the bottom half. However, when reaching into the central sector, the controller reuses the configuration from the previous position (this kind of behavior is common to avoid work space obstacles), and hence the configuration chosen in the central sector is essentially random. While learning succeeds in the top and bottom sectors of the work space, the failure to learn in the central sector is evident from the distorted (black) grid of learned positions.

This convexity problem can be avoided by providing auxiliary variables $\boldsymbol{\xi}$ to the learning component such that the combination $(\mathbf{x}, \boldsymbol{\xi})$ unambiguously specifies the motor state of the system (although identifying such variables in practice can be nontrivial). For example, the discrete redundancy found in the 2dof arm requires a discrete variable $\xi = \pm 1$ to identify the particular arm configuration to be used. This solution is not particularly satisfactory since it breaks modularity, forcing a controller whose task is simply to reach to a given position to take responsibility for choosing the required arm configuration.

More interesting from our point of view, this solution also increases the complexity of the reference structure, since the number K of reference

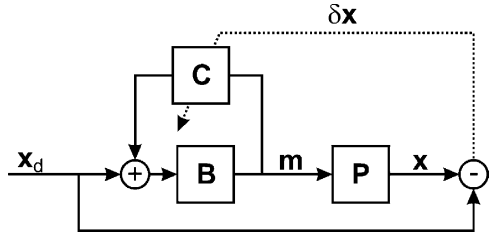

Figure 5: Recurrent architecture. Here the motor command generated by the fixed element **B** is the input to the adaptive element **C**. The output of **C** is then used as a correction to the input to **B**. This loop implements Brindley's (1964) influential suggestion that the cerebellum elaborates commands coming from higher-level structures in the context of information about the current state of the organism. In this recurrent architecture, the sensor error $\delta\mathbf{x}$ becomes effectively proximal to **C** and, as demonstrated in the text, can be used directly as a teaching signal.

matrices required must be further increased to reflect the dependence on the extra parameters $\boldsymbol{\xi}$. For example, to learn correctly in the 2dof arm example in Figure 4b, the two different arm configurations clearly require different reference matrices; hence, to allow both configurations over the whole work space increases the number of hard-wired parameters by a factor of 2 to $2 \times 12 = 24$. Even in this simple example, the complexity of the reference structure required to support learning is beginning to approach that of the structure to be learned.

Note that the situation is not helped by adding a conventional error feedback loop to the adaptive forward architecture (as in the feedback error learning model). This loop also requires a motor error signal, and since error is available only in sensory coordinates, different reference structures are required for different arm configurations.

7 The Recurrent Architecture

As we noted in section 1, the forward architecture just described ignores a major feature, the recurrent connectivity, of the circuitry in which the cerebellar microcircuit is embedded. An alternative recurrent architecture reflecting this connectivity is shown schematically in Figure 5. Although the analysis of recurrent networks and their learning rules can be very complex (e.g., Pearlmutter, 1995) this architecture is an important exception; in particular, we will show that no backpropagation step is required in the learning rule. The analysis proceeds in two stages. First, a plausible cerebellar learning rule is derived by the familiar method of gradient descent. This derivation does not provide a rigorous proof of convergence because it requires a small-weight-error approximation. Second, a Lyapunov function

for the learning rule is derived and used to demonstrate convergence of the learning rule without the need for the small-weight-error approximation.

We are able to simplify the treatment because we deal only with kinematics. Hence, we can idealize the recurrent loop as an algebraic loop in which the output $\mathbf{m}$ of the closed loop shown in Figure 5 satisfies the implicit equation,

$$\mathbf{m} = \mathbf{B}(\mathbf{x}_d + \mathbf{C}(\mathbf{m})). \tag{7.1}$$

Clearly control is possible only if the fixed element $\mathbf{B}$ has some left inverse $\mathbf{B}^{-1}$. Applying this inverse to equation 7.1, we find that the desired position input $\mathbf{x}_d$ is related to the actual motor command $\mathbf{m}$ by the equation

$$\mathbf{x}_d = \mathbf{B}^{-1}(\mathbf{m}) - \mathbf{C}(\mathbf{m}). \tag{7.2}$$

Again, we assume the matching condition so that weights exist for which $\mathbf{C}$ takes the exact value $\mathbf{C}^*$. For this choice of $\mathbf{C}$, the desired position will equal the actual output position, that is,

$$\mathbf{x} = \mathbf{P}(\mathbf{m}) = \mathbf{B}^{-1}(\mathbf{m}) - \mathbf{C}^*(\mathbf{m}), \tag{7.3}$$

from which we derive the following expression for the desired cerebellar filter:

$$\mathbf{C}^* = \mathbf{B}^{-1} - \mathbf{P}. \tag{7.4}$$

By subtracting equation 7.3 from 7.2, we find that $\delta\mathbf{x} = \mathbf{x} - \mathbf{x}_d = \mathbf{C}^*(\mathbf{m}) - \mathbf{C}(\mathbf{m})$, and substituting $\mathbf{C}^* = \sum w_{ij}^* \mathbf{G}_{ij}$, $\mathbf{C} = \sum w_{ij} \mathbf{G}_{ij}$ gives the following simple relationship between sensory error and synaptic weight error:

$$\delta\mathbf{x} = \mathbf{P}(\mathbf{m}) - \mathbf{x}_d = \mathbf{C}(\mathbf{m}) - \mathbf{C}^*(\mathbf{m}) = \sum (w_{ij} - w_{ij}^*)\mathbf{G}_{ij}(\mathbf{m}). \tag{7.5}$$

(This is analogous to equation 4.3 relating motor error and synaptic weight error for the forward architecture.) Although this equation is at first sight linear in the weights w_{ij}, this appearance is misleading since the argument $\mathbf{m}$ also depends implicitly on the w_{ij}. However, the appearance of linearity is close enough to the truth to allow us to derive a simple learning rule.

If weight errors are small, the second term in the derivative,

$$\frac{\partial \delta\mathbf{x}}{\partial w_{ij}} = \mathbf{G}_{ij}(\mathbf{m}) + \sum (w_{kl} - w_{kl}^*) \frac{\partial \mathbf{G}_{kl}(\mathbf{m})}{\partial w_{ij}}, \tag{7.6}$$

can be neglected to give the approximation

$$\frac{\partial \delta \mathbf{x}}{\partial w_{ij}} \approx \mathbf{G}_{ij}(\mathbf{m}). \tag{7.7}$$

Using this result, we can derive an approximate gradient-descent learning rule by minimizing expected square sensory error (rather than motor error, as in the previous section). Defining

$$E_s = \frac{1}{2}\left\langle \delta x^2 \right\rangle = \frac{1}{2}\left\langle \delta \mathbf{x}^t \delta \mathbf{x} \right\rangle, \tag{7.8}$$

its gradient is

$$\frac{\partial E_s}{\partial w_{ij}} = \left\langle \delta \mathbf{x}^t \frac{\partial \delta \mathbf{x}}{\partial w_{ij}} \right\rangle \approx \left\langle \delta \mathbf{x}^t \mathbf{G}_{ij}(\mathbf{m}) \right\rangle = \left\langle \delta x_i \; p_j \right\rangle, \tag{7.9}$$

leading to the approximate gradient-descent learning rule

$$\delta w_{ij} = -\beta \left\langle \delta x_i \; p_j \right\rangle. \tag{7.10}$$

In this learning rule, no Jacobian appears, and hence no reference structures embodying prior knowledge of plant parameters are required. Comparison with the covariance learning rule (see equation 2.4) shows that the teaching signal required on the climbing fibers in recurrent architecture is now the sensory error:

$$e_i = \delta x_i. \tag{7.11}$$

Although this local learning rule has been derived as an approximate gradient-descent rule, its properties are more easily determined by a Lyapunov analysis; this analysis is simplified if we work with the continuous update form of the learning rule:

$$\dot{w}_{ij} = -\beta \, \delta x_i \; p_j. \tag{7.12}$$

As a Lyapunov function, we use the sum square synaptic weight error,

$$V = \frac{1}{2} \sum (w_{ij} - w_{ij}^*)^2, \tag{7.13}$$

which has time derivative

$$\dot{V} = \sum \dot{w}_{ij}(w_{ij} - w_{ij}^*) = -\beta \sum_i \left\langle \delta x_i \sum_j (w_{ij} - w_{ij}^*) p_j \right\rangle. \tag{7.14}$$

Substituting into this expression the expression for sensory error above, we find that

$$\dot{V} = -\beta\delta\mathbf{x}^2. \tag{7.15}$$

Since its derivative is nonpositive, V is a Lyapunov function, that is, a positive function that decreases over time as learning proceeds. It is unnecessary to appeal to the Lyapunov theorems to determine the behavior of this system sufficiently for practical purposes. The equation above shows that over a fixed period of time, the sum square synaptic weight error decreases by an amount proportional to the mean square sensory error; hence, it is clear that the system can make RMS sensory errors above a certain magnitude only for a limited time, since V would otherwise become negative, which is impossible.

8 The Motor Error Problem Is Solved

It is clear that this architecture solves the motor error problem in that there is no longer a need for unavailable motor error signals on the climbing fibers or for complex reference structures to estimate them.

Figure 6a shows the performance of recurrent architecture for the 2dof arm problem described in section 3 (see the appendix for implementation details). It can be seen that the arm now recalibrates successfully over the whole work space. Figure 6b shows the decrease in position error during training; this decrease is stochastic in nature, as would be expected from the approximate stochastic gradient-descent rule. In contrast, Figure 6c shows the monotonic decrease of sum square weight error V during training predicted by the Lyapunov analysis, with the greatest decreases taking place where large errors are made.

9 The Nonconvexity Problem Is Solved

In the recurrent architecture, the nonconvexity problem is easily solved because it does not arise. The adaptive element **C** takes motor commands as input, and its task is to learn to associate them with a corrective output. Since the motor command completely determines the current configuration, there is no ambiguity to be resolved. Although we illustrate this property below for the discrete redundancy of the 2dof arm, the reasoning above clearly applies to both discrete and continuous redundancies.

This property confers remarkable modularity on recurrent architecture. It means that the connectivity of a cerebellar controller is determined solely by the task and is independent of low-level details such as the particular algorithm chosen for resolving joint angle redundancy or how, for example, reciprocal innervation allocates the tension in antagonistic muscle pairs.

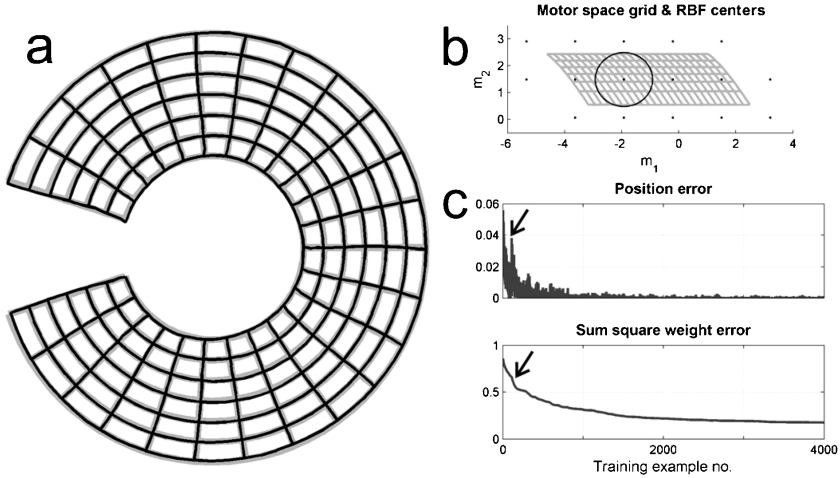

Figure 6: (a) This panel illustrates successful recalibration by the recurrent architecture. After training, the learned (black) grid overlays the exact (gray) grid over the whole work space (compare with the initial performance in Figure 2). Learning rate $\beta = 0.05$. (b) The grid shows the region of motor space corresponding to the robot work space. The dots and the circle indicate RBF centers and the receptive field radius. (c) The two graphs illustrate the stochastic decrease in squared position error (top), same units of length as Figure 2, and the associated monotonic decrease in sum square synaptic weight error (bottom) as predicted by theory. The behavior at the positions marked by arrows illustrates the fact that faster decrease in sum square weight error is associated with larger position error, as predicted by the Lyapunov equation, 7.13.

This property is illustrated in Figure 7a, where the recurrent architecture is applied to the redundant reaching problem described in section 6. It can be seen that learning is now satisfactory over the whole work space. The only modification to the net for the task of Figure 7 is the need for RBF centers covering points in motor space associated with the alternative arm configuration. This grid of RBF centers is shown in Figure 7b. The situation would be only slightly different for a continuous redundancy; in this case, new RBF centers would be needed to cover all points in motor command space accessible by the redundant degrees of freedom.

10 Discussion

As argued in section 1, one reason that cerebellar-inspired models have been of modest use to robotics is that cerebellar connectivity is often poorly understood (Lisberger, 1998). The general idea that identical cerebellar microcircuits can be wired up to perform a wide range of motor and

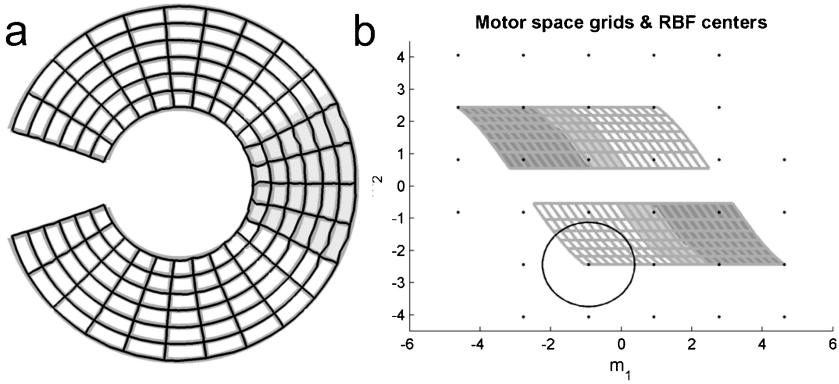

Figure 7: (a) This panel shows that recurrent architecture solves the redundant reaching problem example described in section 6 for which forward architecture fails (compare with Figure 4). The learned (black) grid overlays the exact (gray) grid accurately over the whole work space, including the horizontal 60 degree sector in which both arm configurations are used. Learning rate $\beta = 0.05$. (b) This panel shows the separate grids in motor space associated with the two arm configurations. The grid of dots and the circle indicate the RBF centers and receptive field radius. The dark gray regions highlight motor commands used to generate the arm configurations used consistently in the top and bottom sectors of the work space, and the light gray regions highlight motor commands that generate the two alternative configurations used in the central sector of the work space (the unshaded regions are not used). Since the arm configurations that are ambiguous in task space are represented in separate regions of motor space, they are learned independently in the recurrent architecture.

cognitive functions (Ito, 1984, 1997) is well appreciated, but identifying specific instances has proved difficult. Here we have explored the computational capacities of the cerebellar microcircuit embedded in a recurrent architecture for adaptive feedforward control of nonlinear redundant systems as exemplified by a simulated 2dof robot arm. We have shown that the architecture solves the distal error problem, copes naturally with the redundancy/convexity problem, and gives enhanced modularity. We now compare it with alternative architectures from both computational and biological perspectives

10.1 Computational Control. The distal error problem arises whenever output errors are used to train internal parameters (Jordan, 1996; Jordan & Wolpert, 2000). It is a fundamental obstacle in neural learning systems, and the consequent lack of biological plausibility of learning rules in neural net supervised learning algorithms has become a cliché. There have been two main previous approaches to solving the distal error problem: (1) continue

to use standard architectures and hypothesize the existence of structures implementing the required error backpropagation schemes, or (2) look for those special architectures in which output errors are themselves sufficient for training.

The forward learning architecture (see Figure 3) appears poorly suited for solving the distal error problem. Considerable ingenuity has been expended on the feedback error learning scheme developed by Kawato and coworkers (Gomi & Kawato, 1992, 1993) (for a recent rigorous treatment, see Nakanishi & Schaal, 2004) in order to rescue this architecture, but even so, substantial difficulties remain. In feedback error learning, the adaptive component is embedded in a feedback controller so that the estimated motor error δm^{est} is used as both a training signal and a feedback error term. As we have noted, feedback error learning imposes SPR conditions on the accuracy of the motor error estimate and hence requires complex reference structures for generic redundant and nonlinear systems. There have been theoretical attempts to remove the SPR condition. For example, Miyamura and Kimura (2002) avoid the necessity for SPR at the cost of requiring large gains in the conventional error feedback loop; this is unacceptable in autonomous and biological systems since one of the primary reasons for using adaptive control is to avoid the destabilizing effect of large feedback gains given inevitable feedback delays. Despite the difficulties we have noted here, feedback error learning has been usefully applied to online learning by autonomous robots in numerous contexts (e.g., Dean, Mayhew, Thacker, & Langdon, 1991; Mayhew, Zheng, & Cornell, 1992). It is clear that feedback error learning remains a useful approach for problems in which simplifying features of the motor plant mean that the reference structures are easily estimated.

We have presented a general architecture for tracking control in which output error can be used directly for training. Other architectures of this type in the literature have been designed for specific control problems. For example, the adaptive scheme for control of robot manipulators proposed by Slotine and Li (1989) relies on special features of the problem of controlling joint angles using joint torques. We note also the adaptive schemes for particular single-input–single-output nonlinear systems considered by Patino and Liu (2000) and Nakanishi and Schaal (2004). Although none of these architectures tackles the generic problems of nonlinearity and redundancy considered here, it is interesting to note that they also use recurrent architectures in an essential way, supporting the idea that recurrent connectivity may play a fundamental role in simplifying biological motor control.

10.2 Biological Plausibility. From a biological perspective, the recurrent architecture appears more plausible in the context of plant compensation than the forward architecture, with its requirements for feedback error learning, for three reasons.

First, as pointed out in section 1, anatomical evidence indicates that the recurrent architecture is a feature of many cerebellar microzones. In addition, where it is available, electrophysiological evidence has specifically identified efferent-copy information as part of the mossy fiber input to particular regions of the cerebellum. Important examples are (1) the primate flocculus and ventral paraflocculus, responsible for adaptation of the vestibulo-ocular reflex (VOR), where extensive recordings have shown that about three-quarters of their mossy fiber inputs carry eye-movement-related signals (Miles, Fuller, Braitman, & Dow, 1980); (2) the oculomotor vermis, responsible for saccadic adaptation, where about 25% of mossy fibers show short-latency burst firing in association with saccades that closely resemble the activity of excitatory burst neurons in the paramedian pontine reticular formation (Ohtsuka & Noda, 1992); and (3) regions of cerebellar cortex associated with control of limb movement by the red nucleus receive an efferent copy of rubrospinal output to cerebellum, related to limb position and velocity (Keifer & Houk, 1994). Thus, the defining feature of the recurrent architecture used here appears to be present for all the cerebellar microzones that have been adequately investigated.

Second, the recurrent architecture allows use of sensory error signals, that is, the sensory consequences of inaccurate motor commands, which are physically available signals. Previous inability to use such distal error signals has been a fundamental obstacle in neural learning systems, so that architectures such as the one described here, in which distal error can be used directly as a teaching signal, have fundamental importance as basic components of biological learning systems. Hence, if the recurrent architecture were used biologically, we would expect cerebellar climbing fibers to carry sensory information. In contrast, a central consequence of feedback error learning is the identification of climbing fiber signals with motor error. In the words of Gomi and Kawato (1992), "Our view that the climbing fibers carry control error information, the difference between the instructions and the motor act, is common to most cerebellar motor-learning models; however ours is unique in that this error information is represented in motor-command coordinates." This view runs into both theoretical and empirical problems.

From a theoretical point of view, the use of the motor error signal requires not only new and as yet unidentified neural reference structures to recover motor error from observable sensory errors, but also new and as yet unidentified mechanisms to calibrate these structures. Again in the words of Gomi and Kawato (1992), "The most interesting and challenging theoretical problem [raised by FEL] is setting an appropriate inverse reference model in the feedback controller at the spinal and brainstem levels."

From the point of view of experimental evidence, it appears that many climbing fibers are in fact strongly activated by sensory inputs, such as touch, pain, muscle sense, or, in the case of the VOR, retinal slip (e.g., Apps & Garwicz, 2005; De Zeeuw et al., 1998; Simpson, Wylie, & De Zeeuw, 1996).

In certain cases where nonsensory signals have been identified in climbing-fiber discharge (e.g., Andersson, Garwicz, & Hesslow, 1988; Gibson, Horn, & Pong, 2002), their effect seems to be to emphasize the unpredicted sensory consequences of a movement by gating the expected consequences. Such gated signals are still physically available sensory signals. In other instances, for example, retinal slip in the horizontal VOR, it appears that the effect of nonsensory modulation is to produce a two-valued slip signal that conveys information about the direction of image movement but not its speed (Highstein, Porrill, & Dean, 2005; Simpson, Belton, Suh, & Winkelman, 2002). One line of evidence often used to support feedback error learning concerns ocular following, where externally imposed slip-like movements of the retinal image drive compensatory eye movements. It has been shown that the associated complex spike discharge in the flocculus can be predicted from either slip or eye movement signals (Kobayashi et al., 1998). However, given that a later article states that "only the velocity of the retinal error (retinal slip) was statistically sufficient" (Yamamoto, Kobayashi, Takemura, Kawano, & Kawato, 2002, p. 1558) to reproduce the observed variability in climbing fiber discharge, it is not clear that this evidence decisively supports the existence of a motor error signal, even in these special and ambiguous circumstances.

Although we have not considered dynamics here, a further advantage of the recurrent architecture is its capacity to generate long-time constant signals when plant compensation requires integrator-like processes (Dean et al., 2002; Porrill et al., 2004). This desirable feature of the recurrent architecture was pointed out for eye-position control by Galiana and Outerbridge (1984) and has been incorporated in other models of gaze holding (e.g., Glasauer, 2003). It is unclear how forward architectures could be used to achieve the observed performance of the neural integrator (Robinson, 1974).

10.3 Further Developments. Our previous work on plant compensation in the VOR (Dean et al., 2002; Porrill et al., 2004) established the capabilities of recurrent architecture for dynamic control of linear systems. Here we have extended these results to the kinematic control of redundant and nonlinear systems. It is clearly a priority to extend these results to dynamic nonlinear control problems. It is also important to implement the decorrelation-control scheme in a robot, and this work is currently in progress.

We have emphasized the limitations of the feedback-error-learning architecture, but its combination of feedback and feedforward controllers does offer considerable advantages for robust online control. It appears that a possibly similar strategy is used biologically to control gaze stability, combining the optokinetic (feedback) and vestibulo-ocular (feedforward) reflexes (Carpenter, 1988). As we will show elsewhere, the recurrent architecture can also be embedded stably and naturally in a conventional feedback loop.

Finally, although the recurrent architecture does not need forward connections for plant compensation (and so they are not shown in Figure 5), such connections are also ubiquitous for cerebellar microzones. We conjecture that once plant compensation has been achieved, a microzone could in principle use these inputs for a wide range of purposes, including sensory calibration and predictive control.

Appendix: Technical Details

Explicit details of the forward and recurrent algorithms for the robotic application are supplied below. This is a vanilla RBF implementation, since our intention is to concentrate on the nature of the error signal and the learning rule. Both accuracy and learning speed could be greatly improved by optimizing the choice of centers and transforming to an optimal basis of receptive fields.

The forward kinematics for the 2dof robot arm with arm lengths (l_1, l_2) is given by

$$\begin{aligned} x_1 &= P_1(m_1, m_2) = l_1 \cos m_1 + l_2 \cos(m_1 + m_2) \\ x_2 &= P_2(m_1, m_2) = l_1 \sin m_1 + l_2 \sin(m_1 + m_2). \end{aligned} \tag{A.1}$$

The brainstem component of the controller is defined as the exact inverse kinematics for a robot with slightly different arm lengths (l_1', l_2'),

$$\begin{aligned} m_1 &= B_1(x_1, x_2) = \tan^{-1}\left(\frac{x_2}{x_1}\right) - \tan^{-1}\left(\frac{l_2' \sin \xi\theta}{l_1' + l_2' \sin \xi\theta}\right) \\ m_2 &= B_2(x_1, x_2) = \xi\theta, \end{aligned} \tag{A.2}$$

where

$$\theta = \cos^{-1}\left(\frac{x_1^2 + x_1^2 - l_1'^2 - l_2'^2}{2l_1'l_2'}\right), \tag{A.3}$$

and the choice of $\xi = \pm 1$ determines the arm configuration.

In the forward architecture, the parallel fiber signals are given by gaussian RBFs

$$p_j = G_j(x_1, x_2) = e^{-\frac{1}{2\sigma^2}\left((x_1 - c_{1j})^2 + (x_2 - c_{2j})^2\right)}, \tag{A.4}$$

with the centers (c_{1j}, c_{2j}) chosen on a rectangular grid covering the work space and with σ equal to $2^{1/2}$ times the maximum grid spacing (see Figure 4). The forward architecture implies the following expression for

the motor commands:

$$m_1 = B_1(x_1, x_2) + \sum w_{1j}\, p_j$$
$$m_2 = B_2(x_1, x_2) + \sum w_{2j}\, p_j. \tag{A.5}$$

The unknown weights w_{ij} were initially set to 0. The two components of sensory error are given by the formula

$$\delta x_1 = P_1\,(m_1, m_2) - x_1$$
$$\delta x_2 = P_2(m_1, m_2) - x_2, \tag{A.6}$$

from which the two components of motor error are estimated using a 2×2 reference matrix R

$$\begin{pmatrix} \delta m_1^{est} \\ \delta m_2^{est} \end{pmatrix} = \begin{pmatrix} R_{11} & R_{12} \\ R_{21} & R_{22} \end{pmatrix} \begin{pmatrix} \delta x_1 \\ \delta x_2 \end{pmatrix}. \tag{A.7}$$

RBF weights are updated using the learning rule

$$w_{ij}^{new} = w_{ij}^{old} - \beta \delta m_i^{est}\, p_j. \tag{A.8}$$

In the alternative recurrent architecture, the PF signals are given by RBFs,

$$p_j = G_j(m_1, m_2) = e^{-\frac{1}{2\sigma^2}\left((m_1 - c_{1j})^2 + (m_2 - c_{2j})^2\right)}, \tag{A.9}$$

with centers chosen on a rectangular grid in motor space. The grid was chosen to cover the image of the work space in motor space (see Figure 6b). The recurrent architecture of Figure 5 implies the following equation for motor commands

$$m_1 = B_1\left(x_1 + \sum w_{1j}\, p_j,\ x_2 + \sum w_{2j}\, p_j\right)$$
$$m_2 = B_2\left(x_2 + \sum w_{1j}\, p_j,\ x_2 + \sum w_{2j}\, p_j\right). \tag{A.10}$$

This is an implicit equation for motor error since the p_j depend on the m_i via equation A.6. Its solution was obtained at each trial by iterating $\mathbf{m}_{n+1} = \mathbf{B}(\mathbf{x} + \mathbf{C}(\mathbf{m}_n))$ to convergence (a relative accuracy of 10^{-4} required at most 10 iterations in the simulations reported here). This off-line iteration is necessary to allow the arm to make discontinuous movements between randomly chosen gridpoints. If waypoints $\mathbf{x}_n$ are closely sampled from a continuous curve, the more natural alternative online procedure $\mathbf{m}_{n+1} = \mathbf{B}(\mathbf{x}_n + \mathbf{C}(\mathbf{m}_n))$ can be used.

Again the unknown weights w_{ij} were initially set to 0. Sensory error obtained from equation A.3 above was used directly in the learning rule

$$w_{ij}^{new} = w_{ij}^{old} - \beta \delta x_i p_j. \tag{A.11}$$

Values for the optimal weight values w_{ij}^* are required to calculate the sum square weight errors plotted in Figure 6. These were obtained by direct batch minimization of sum square reaching error calculated over a subsampled grid of points in the work space.

We have primarily investigated convergence in the circumstances in which it is believed to operate biologically, that is, in repair shop mode with changes in plant characteristics of 10% to 15%. However, simulations have indicated that it also converges from initial weights corresponding to grossly degraded performance, although we have not investigated this systematically.

Acknowledgments

This work was supported by EPSRC grant GR/T10602/01 under their Novel Computation Initiative.

References

Albus, J. S. (1971). A theory of cerebellar function. *Mathematical Biosciences, 10*, 25–61.

Andersson, G., Garwicz, M., & Hesslow, G. (1988). Evidence for a GABA-mediated cerebellar inhibition of the inferior olive in the cat. *Experimental Brain Research, 72*, 450–456.

Apps, R., & Garwicz, M. (2005). Anatomical and physiological foundations of cerebellar information processing. *Nature Reviews Neuroscience, 6*(4), 297–311.

Boyden, E. S., Katoh, A., & Raymond, J. L. (2004). Cerebellum-dependent learning: The role of multiple plasticity mechanisms. *Annual Review of Neuroscience, 27*, 581–609.

Brindley, G. S. (1964). The use made by the cerebellum of the information that it receives from sense organs. *International Brain Research Organization Bulletin, 3*, 80.

Carpenter, R. H. S. (1988). *Movements of the eyes* (2nd ed.). London: Pion.

De Zeeuw, C. I., Simpson, J. I., Hoogenraad, C. C., Galjart, N., Koekkoek, S. K. E., & Ruigrok, T. J. H. (1998). Microcircuitry and function of the inferior olive. *Trends in Neurosciences, 21*(9), 391–400.

Dean, P., Mayhew, J. E. W., Thacker, N., & Langdon, P. M. (1991). Saccade control in a simulated robot camera-head system: Neural net architectures for efficient learning of inverse kinematics. *Biological Cybernetics, 66*, 27–36.

Dean, P., Porrill, J., & Stone, J. V. (2002). Decorrelation control by the cerebellum achieves oculomotor plant compensation in simulated vestibulo-ocular reflex. *Proceedings of the Royal Society of London, Series B, 269*(1503), 1895–1904.

Dean, P., Porrill, J., & Stone, J. V. (2004). Visual awareness and the cerebellum: Possible role of decorrelation control. *Progress in Brain Research, 144*, 61–75.

Eccles, J. C., Ito, M., & Szentágothai, J. (1967). *The cerebellum as a neuronal machine*. Berlin: Springer-Verlag.

Fujita, M. (1982). Adaptive filter model of the cerebellum. *Biological Cybernetics, 45*, 195–206.

Galiana, H. L., & Outerbridge, J. S. (1984). A bilateral model for central neural pathways in vestibuloocular reflex. *Journal of Neurophysiology, 51*(2), 210–241.

Gibson, A. R., Horn, K. M., & Pong, M. (2002). Inhibitory control of olivary discharge. *Annals of the New York Academy of Sciences, 978*, 219–231.

Glasauer, S. (2003). Cerebellar contribution to saccades and gaze holding—a modeling approach. *Annals of the New York Academy of Sciences, 1004*, 206–219.

Gomi, H., & Kawato, M. (1992). Adaptive feedback control models of the vestibulocerebellum and spinocerebellum. *Biological Cybernetics, 68*(2), 105–114.

Gomi, H., & Kawato, M. (1993). Neural network control for a closed-loop system using feedback-error-learning. *Neural Networks, 6*, 933–946.

Highstein, S. M., Porrill, J., & Dean, P. (2005). Report on a workshop concerning the cerebellum and motor learning. Held in St Louis October 2004. *Cerebellum, 4*, 1–11.

Ito, M. (1970). Neurophysiological aspects of the cerebellar motor control system. *International Journal of Neurology (Montevideo), 7*, 162–176.

Ito, M. (1984). *The cerebellum and neural control*. New York: Raven Press.

Ito, M. (1997). Cerebellar microcomplexes. *International Review of Neurobiology, 41*, 475–487.

Jordan, M. I. (1996). Computational aspects of motor control and motor learning. In H. Heuer & S. Keele (Eds.), *Handbook of perception and action, Vol. 2: Motor skills* (pp. 71–120). London: Academic Press.

Jordan, M. I., & Wolpert, D. M. (2000). Computational motor control. In M. S. Gazzaniga (Ed.), *The new cognitive neurosciences* (2nd ed., pp. 601–618). Cambridge MA: MIT Press.

Keifer, J., & Houk, J. C. (1994). Motor function of the cerebellorubrospinal system. *Physiological Reviews, 74*(3), 509–542.

Kelly, R. M., & Strick, P. L. (2003). Cerebellar loops with motor cortex and prefrontal cortex of a nonhuman primate. *Journal of Neuroscience, 23*(23), 8432–8444.

Kobayashi, Y., Kawano, K., Takemura, A., Inoue, Y., Kitama, T., Gomi, H., & Kawato, M. (1998). Temporal firing patterns of Purkinje cells in the cerebellar ventral paraflocculus during ocular following responses in monkeys II. Complex spikes. *Journal of Neurophysiology, 80*(2), 832–848.

Lisberger, S. G. (1998). Cerebellar LTD: A molecular mechanism of behavioral learning? *Cell, 92*(6), 701–704.

Marr, D. (1969). A theory of cerebellar cortex. *Journal of Physiology, 202*, 437–470.

Marr, D. (1982). *Vision: A computational investigation into the human representation and processing of visual information*. San Francisco: Freeman.

Mayhew, J. E. W., Zheng, Y., & Cornell, S. (1992). The adaptive control of a four-degrees-of-freedom stereo camera head. *Philosophical Transactions of the Royal Society of London, Series B, 337*, 315–326.

Miles, F. A., Fuller, J. H., Braitman, D. J., & Dow, B. M. (1980). Long-term adaptive changes in primate vestibuloocular reflex. III. Electrophysiological observations in flocculus of normal monkeys. *Journal of Neurophysiology, 43*, 1437–1476.

Miyamura, A., & Kimura, H. (2002). Stability of feedback error learning scheme. *Systems and Control Letters, 45*, 303–316.

Nakanishi, J., & Schaal, S. (2004). Feedback error learning and nonlinear adaptive control. *Neural Networks, 17*(10), 1453–1465.

Ohtsuka, K., & Noda, H. (1992). Burst discharges of mossy fibers in the oculomotor vermis of macaque monkeys during saccadic eye movements. *Neuroscience Research, 15*(1–2), 102–114.

Patino, H. D., & Liu, D. (2000). Neural network–based model reference adaptive control system. *IEEE Transactions on Systems, Man and Cybernetics—Part B: Cybernetics, 30*, 198–203.

Pearlmutter, B. A. (1995). Gradient calculations for dynamic recurrent neural networks. *IEEE Transactions on Neural Networks, 6*(5), 1212–1228.

Porrill, J., & Dean, P. (2004). Recurrent cerebellar loops simplify adaptive control of redundant and nonlinear motor systems. In *2004 Abstract Viewer/Itinerary Planner* (pp. Prog. No. 989.984). Washington, DC: Society for Neuroscience.

Porrill, J., Dean, P., & Stone, J. V. (2004). Recurrent cerebellar architecture solves the motor error problem. *Proceedings of the Royal Society of London, Series B, 271*, 789–796.

Robinson, D. A. (1974). The effect of cerebellectomy on the cat's vestibulo-ocular integrator. *Brain Research, 71*, 195–207.

Sejnowski, T. J. (1977). Storing covariance with nonlinearly interacting neurons. *Journal of Mathematical Biology, 4*, 303–321.

Simpson, J. I., Belton, T., Suh, M., & Winkelman, B. (2002). Complex spike activity in the flocculus signals more than the eye can see. *Annals of the New York Academy of Sciences, 978*, 232–236.

Simpson, J. I., Wylie, D. R., & De Zeeuw, C. I. (1996). On climbing fiber signals and their consequence(s). *Behavioral and Brain Sciences, 19*(3), 384–398.

Slotine, J. J. E., & Li, W. P. (1989). Composite adaptive-control of robot manipulators. *Automatica, 25*(4), 509–519.

Widrow, B., & Stearns, S. D. (1985). *Adaptive signal processing*. Upper Saddle River, NJ: Prentice Hall.

Yamamoto, K., Kobayashi, Y., Takemura, A., Kawano, K., & Kawato, M. (2002). Computational studies on acquisition and adaptation of ocular following responses based on cerebellar synaptic plasticity. *Journal of Neurophysiology, 87*(3), 1554–1571.

Received August 8, 2005; accepted May 30, 2006.